Rev.Adv.Mater.Sci. 20(2009) 113-124

PHYSICS OF GRANULAR MATTER: PATTERN FORMATION AND APPLICATIONS

Christof A. Kruelle[1,2]

[1]Experimentalphysik V, Universität Bayreuth, D-95440 Bayreuth, Germany
[2]Maschinenbau und Mechatronik, Hochschule Karlsruhe, D-72133, Karlsruhe Germany

Received: February 03, 2008

Abstract. A summary of results is presented from experiments in granular systems, which are excited by vertical and/or horizontal vibrations. The transitions between different dynamic states depend on internal properties of the granular system like the density of particles and on external parameters of the driving shakers. Characteristic for granular systems are such counterintuitive phenomena as the crystallization by increasing the vibration amplitude and thereby the energy input, or the rise of large particles in a sea of smaller ones (Brazil-nut effect). For horizontal shaking of a binary system the demixing of small and large particles is found to occur at the same critical particle density as the liquid-solid transition. The combined action of both vertical and horizontal vibrations for the controlled transport of bulk solids is utilized already for a long time in industrial applications. In a certain driving range it is known that standing surface waves occur at half the forcing frequency. The three experiments presented here indicate that the four major concepts describing the complex behavior of a vibrated granular system, namely phase transition, segregation, pattern formation, and transport are closely related and yield a rewarding field for future research.

1. INTRODUCTION

An accumulation of macroscopic grains, set in motion by an external driving force, can show surprising behavior (for examples, see Fig. 1). A peculiar phenomenon - called segregation - occurs as soon as heterogeneous particles are implied, in geophysical rock avalanches as well as in processed powders in the food or chemical industry [1,2]. This de-mixing of grains which differ in size, density, or surface properties, has been intensively studied since the 1990s in laboratory experiments, e.g. in rotating drums [3] and under vertical [4] or, more recently, horizontal linear [5] excitation. Another phenomenon frequently encountered when handling granular material is the transition from a disordered phase to a more organized state, when the density of grains is increased beyond a critical value. This can be observed, for instance, in monodisperse particles under vertical vibration without gravity [6] or under horizontal translational excitation [7].

In this brief review we report on experimental investigations of both phase transitions and segregation phenomena in granular systems, which are agitated by three different vibration exciters. When the particles are externally forced to perform stochastic movements a “granular temperature” can be defined as mean kinetic energy in the center-of-mass system. For describing the physical properties of this ensemble one can ask, in analogy to thermodynamic phase transitions:

- Are there critical temperatures at which the internal structure undergoes qualitative changes?
- Which order parameters characterize the dynamics of the transition?
- What are the consequences for granular mixtures?

Corresponding author: Christof A. Kruelle, e-mail: christof.kruelle@hs-karlsruhe.de

Fig. 1. (a) Sand dune decorated with aeolian ripples, Great Sand Dunes National Monument, Colorado, USA, (b) Oscillating granular surface wave on a vibratory conveyor.

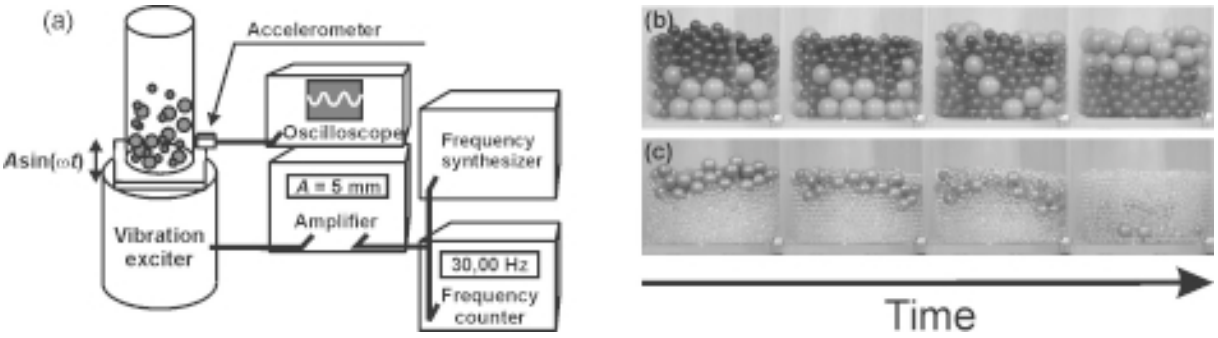

Fig. 2. (a) Sketchy representation of the experimental device for the vertical vibration of a binary mixture of spheres. The container diameter is 9.4 cm. Temporal evolution of (b) initially 8 mm glass beads on top of 15 mm polypropylene, which show the classical Brazil-nut effect and (c) 10 mm bronze spheres on 4 mm glass beads showing the reverse Brazil-nut effect.

2. VERTICAL VIBRATION

Granular media consisting of small and large particles tend to de-mix when shaken vigorously enough. The “Brazil-nut effect” - if a particle mixture is shaken *vertically*, the larger particles will end up on top of the smaller ones, like the nuts in a muesli package - became some kind of *Drosophila melanogaster* of granular media research [4,8-11]. Numerical simulations could validate the rise of larger particles [12,13]. Proposed mechanisms are, for example, convective motion of the smaller particles, which drag the larger ones to the top [9], or the filling of voids by the small particles, thereby lifting the larger ones [4,12,13]. Contrary to these common observations Shinbrot *et al.* [14], however, noticed that a large particle, depending on its density, could also sink to the bottom of the container. Recent theoretical investigations [15-17] explained that either effects, the rise or descend of the larger particles, may occur. The latter case has become known as “reverse Brazil-nut effect”. The borderline between both effects has been predicted by Hong, Quinn, and Luding [15] in a simple relation between the size d_l/d_s and mass ratios m_l/m_s of the large and small particles.

One approach to describe an externally driven granular medium is to consider the individual particles as hard spheres. The driving could be - as in the case of the Brazil-nut effect - a vertical vibration of the container, which confines the granules. For strong driving, where all particles are in continuous motion, the ideas of the kinetic theory of gases can be applied. Then it is possible to define a granular temperature T in analogy to a gas, using the mean kinetic energy:

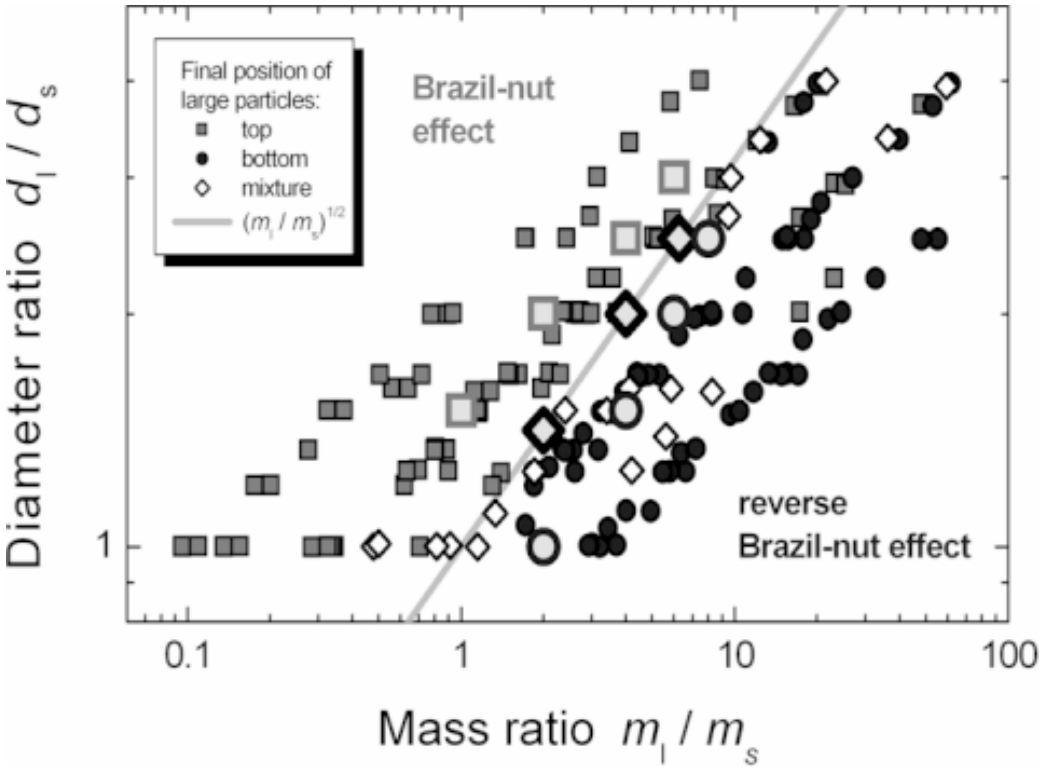

Fig. 3. Phase space for particle properties. The plot shows the regimes where reversed and classical Brazil-nut effects occur depending on the particle properties. Each small symbol represents one of 178 experiments. The solid line separating both areas is given by Eq. (2). The large symbols indicate the prediction of 3D molecular-dynamics simulations performed by Hong *et al*. [15] with up to 3600 particles.

$$\propto \frac{1}{N}\sum_i \frac{m_1}{2}\left(v_i - \langle v\rangle\right)^2, \text{ with}$$
$$\langle v\rangle = \frac{1}{N}\sum_i v_i, \qquad (1)$$

where N is the total number of particles, and m_i and v_i are the mass and the velocity of the i-th particle, respectively. Hong [18] calculated, on the basis of this model, a critical granular temperature $T_c = mgd\mu/\mu_0$, below which a system of monodisperse spheres condensates. This critical temperature depends on the diameter d of the particles and the initial filling height μ, measured in units of d. Here g denotes the gravitational acceleration and μ_0 is a constant, which depends on the spatial dimension and the underlying packing structure [18].

For a binary particle mixture different critical temperatures do exist, as pointed out by Hong *et al.* [15]. If a binary mixture of spheres is agitated by an external shaker, such that the granular temperature is in between the two critical values, one type of particle condensates while the other remains fluidized. It depends on the size and mass of the particles, which particle species will condensate and therefore sink to the bottom of the container. Following Rosato *et al.* [12], Hong *et al.* claimed that the cross-over condition is given when the ratio of the critical temperatures is equal to the volume ratio of the two particle species, which leads, in D dimensions, to the simple relation

$$\frac{d_l}{d_s} = \left(\frac{m_l}{m_s}\right)^{\frac{1}{D-1}}. \qquad (2)$$

If, in 3D, the diameter ratio is larger than the square root of the mass ratio, the particle mixture should show Brazil-nut effect and vice versa.

The prediction of Eq. (2) was put to the test [19] by preparing an instable layering, followed by a controlled shaking of the container. Our experimental device (see Fig. 2a) operates at frequencies f between 0 and 100 Hz and normalized accelera-

tions $\Gamma = A(2\pi f)^2/g$ up to 40, where A is the shaking amplitude and g the gravitational acceleration. The acceleration Γ is measured with an accelerometer attached to the base plate of the Perspex cylinder. The granular materials used were spherical particles of various densities and diameters.

In order to check whether a binary mixture would show Brazil-nut behavior or its reverse, we prepared a presumed instable configuration, i.e., we put several layers of the type, which were predicted by Eq. (2) to rise during shaking on the bottom of the Perspex vessel. On top of these we placed one or more layers of the second type. If the prediction was correct, we would observe that the particles on top started to move through the layers of the other particle type, ending up at the bottom of the vessel (see Figs. 2b and 2c). On the other hand, if the prediction turned out to be wrong the initial layering would be stable.

Most experiments have shown clearly either the Brazil-nut effect (Fig. 2b) or the reverse form (Fig. 2c). For some particle combinations, a mixed state was stable. An overview of the experimental results as well as numerical simulations by Hong, Quinn, and Luding [15] together with their theoretical borderline are shown in Fig. 3. For 81% of the tested combinations (145 out of 178) the prediction of Eq. (2) was correct. The prediction failed when one particle type was made of aluminum or polyurethane. We assume that for these materials the condition of hard spheres, which is one of the main propositions in the theory, was not met. We also noticed that, in the case of the reverse Brazil-nut effect, it is crucial to choose an appropriate filling height. It turned out that the effect is completely destroyed if the initially lower layer is too large.

We currently focus on experimental verifications of the premise of this segregation mechanism via condensation. If, at a fixed external driving, a monodisperse set of glass beads exceeds a critical number of particles a phase transition can be observed from a fluidized “gas-like” state to a condensed “crystalline” state. Systematic studies of the dependence of the condensation temperature T_c on the internal parameters (number, size, and material density of the spheres) as well as the external conditions (amplitude and frequency of the shaker) are promising [20].

3. HORIZONTAL CIRCULAR VIBRATION

In this section we present a model system, consisting of two species of glass beads with different size rolling in a horizontal shaker, where both phenomena, segregation and phase transition, are found to be closely related since they occur at about the same granular density [21].

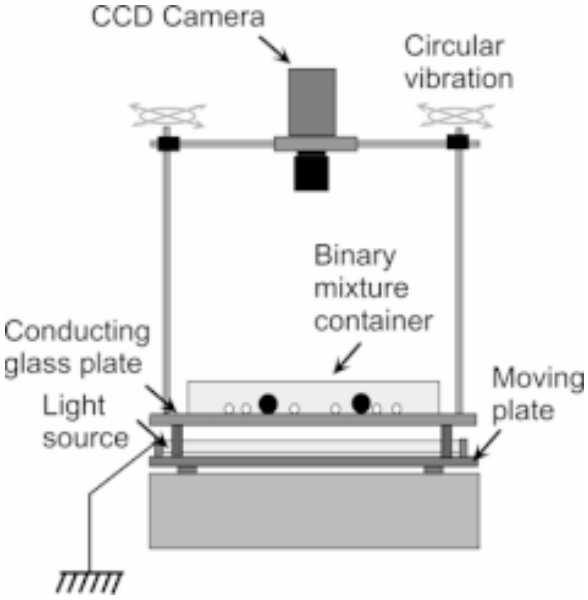

Fig. 4. Sketchy representation of the experimental device for the horizontal circular vibration of a monolayer of glass beads. The container diameter is 29 cm. The bottom glass plate is coated with an electrically conducting indium-tin oxide layer to suppress static electricity.

A sketch of our experimental device is shown in Fig. 4. The particles in the dish are excited in a *horizontal circular vibration*, i.e. a circular movement of the entire platform due to the superposition of two sinusoidal vibrations in perpendicular directions. The frequency f of the table motion can be tuned from 0.5 to 2.0 Hz, with a preset amplitude $A = n/8 \cdot 2.54$ cm, where n=2,…8. The granular system is composed of a variable number, N, of spheres with diameters d= 0.4 or 1.0 cm. To obtain a size-independent control parameter the filling fraction m is defined as the total cross-sectional area $N \cdot \pi(d/2)^2$ of all spheres divided by the surface $\pi(D/2)^2$ of the cell with diameter D = 29 cm. During the motion, the positions of all particles are captured with a charge-coupled-device (CCD) camera fixed to the moving table.

During the experiments we noticed global changes in the dynamics of the system while crossing a critical threshold of the filling fraction μ. In particular, the spheres became arranged in regular, triangular patches. To study this phenomenon,

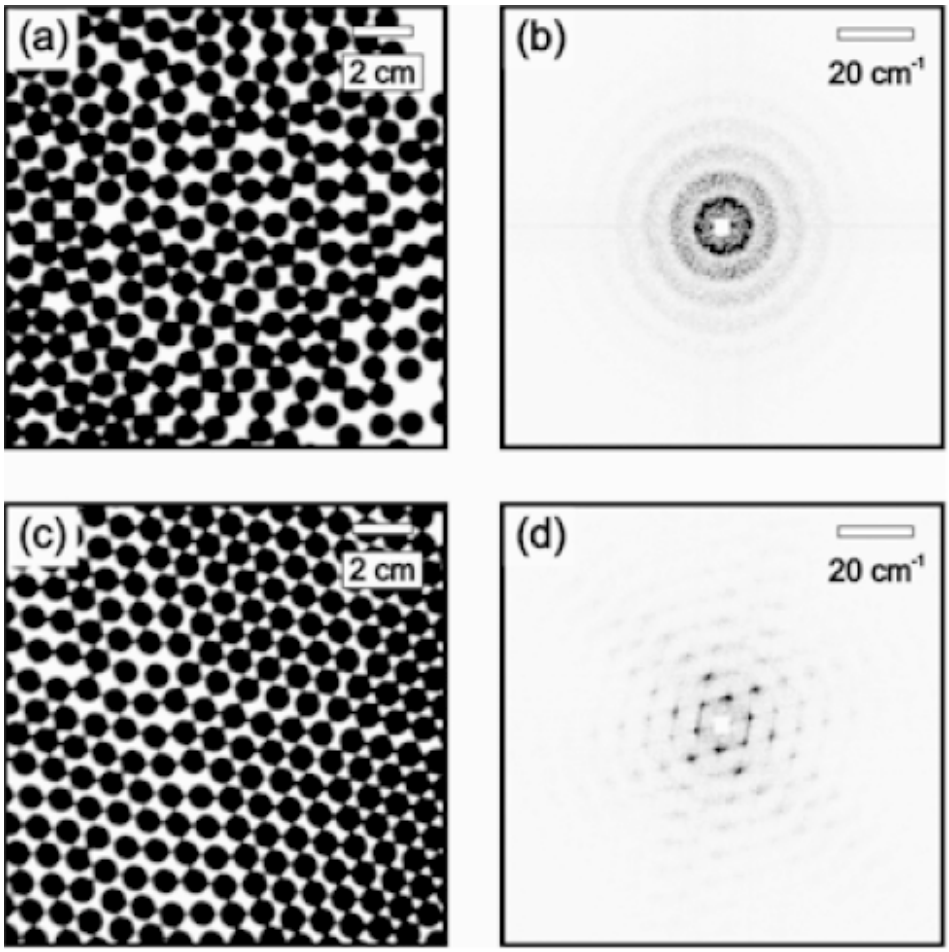

Fig. 5. (a) Image of a monolayer of 410 spheres (filling fraction $\mu = 0.49$) rolling on a table shaken with an amplitude A= 2.22 cm and a frequency f = 1.67 Hz. (b) Contour plot of the corresponding 2D power spectrum. (c) Image of a monolayer of 580 spheres (μ= 0.69) under the same excitation, and (d) its 2D power spectrum. The snapshots are taken in a square of 15 cm at the center of the cell.

a monolayer of *monodisperse* glass spheres is placed inside the dish. After an early stage, during which the system loses all traces of the arbitrary initial configuration, an image is taken. To underline the developed structured state a 2D Fourier transformation (FFT) is performed. Results of these measurements are shown in Fig. 5, for low and high filling fractions of spheres.

At low density, the configuration of grains does not show any structures. Its 2D power spectrum displays a continuous intensity distribution within a circle of radius $k_d = 2\pi/d$. In contrast, at high density, the small spheres arrange in a triangular lattice. In the 2D power spectrum six peaks appear at a wave number $k_0 = 2\pi / (\sqrt{3} / 2)d$, evenly spaced by an angle of $\pi/3$.

The dynamics of the particles is obviously different in these two regimes. At low density each particle is free to follow its own trajectory until it collides with its neighbor, like in a fluid. On the other hand, at high density, the particles are forced into a collective motion inside a 2D crystal. The crossover between these two regimes is reminiscent of a liquid-solid transition. To specify the transition point, a characteristic order parameter is extracted from the power spectra. The spectral intensity is integrated radially in an annulus $0.98k_0<k<1.02k_0$ around the expected peaks. The resulting averaged intensity defines a function of the azimuthal angle φ. In the structured state this function is supposed to present six equidistant peaks.

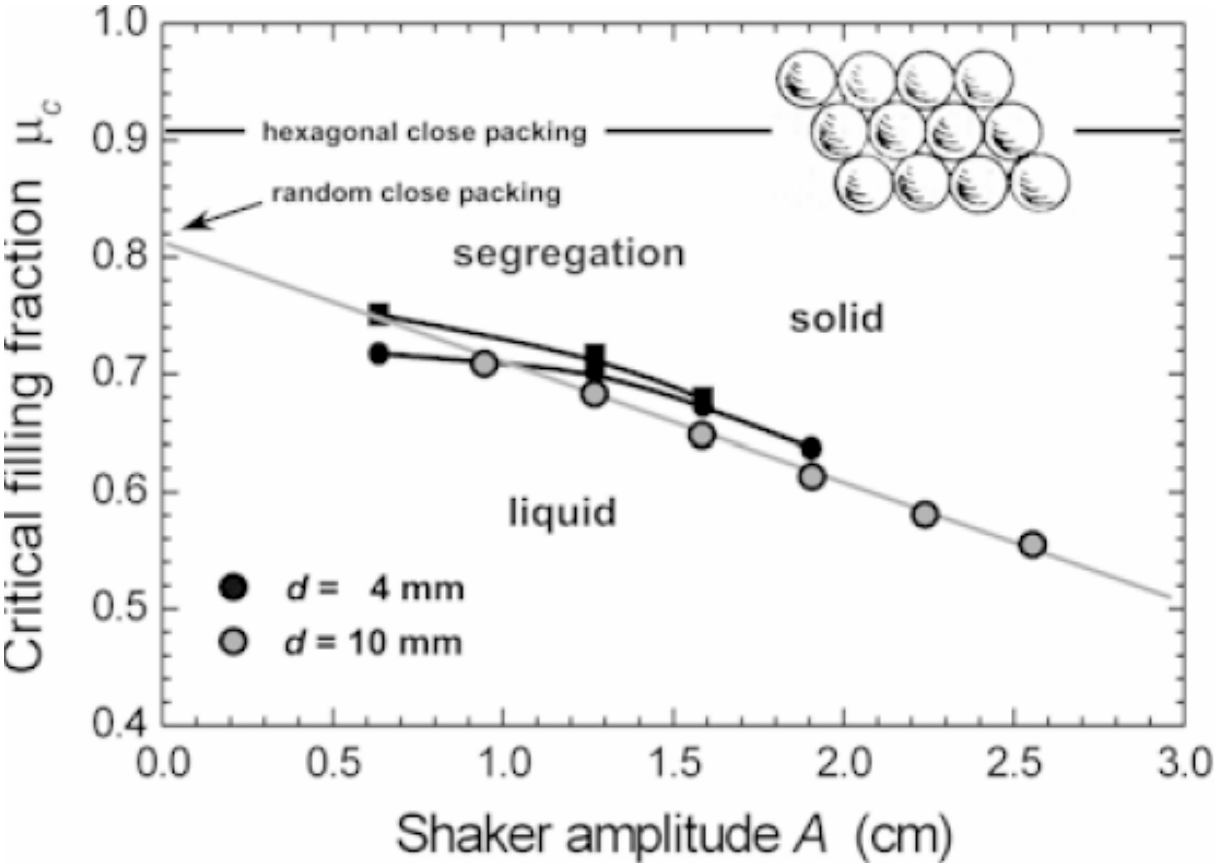

Fig. 6. Phase diagram of the critical filling fraction μ_c vs. shaker amplitude A showing the regime $\mu > \mu_{c,seg}$ (squares), where segregation occurs. The liquid-solid transition line $\mu > \mu_{c,ls}$ (circles) is obtained from the normalized Fourier intensity data for two different particle sizes. The inset shows Johannes Kepler's original drawing of a 2D hexagonal close packing [40].

To obtain a *single* characteristic number, which quantifies the order of the structured state, the angular space $[0,2\pi]$ is subdivided into six equal parts. The intensities in each interval are summed up yielding a singly peaked function $I(\varphi)$ in the reduced angular range $\varphi \in [0,\pi/3]$. Dividing $I(\varphi)$ by its arithmetic mean yields a normalized intensity

$$I_n(\varphi) = \frac{I(\varphi_i)}{\frac{1}{i_{\max}} \sum_{i=1}^{i_{\max}} I(\varphi_i)}, \qquad \varphi_i = i \cdot \frac{\pi}{3 i_{\max}}, \quad i_{\max} = 12, \tag{3}$$

from which an order parameter $\alpha = I_{n,\max}$-1 is derived. The dependence of this quantity a on the filling fraction m is highly nonlinear. A *liquid-solid like* transition can be observed around a critical filling fraction $\mu_{c,ls}$.

For the segregation experiments, a binary mixture of glass beads consisting of 19 large particles of diameter d_l = 1.0 cm imbedded in a variable number of small spheres with diameter d_s = 0.4 cm are prepared. Initially the large spheres are placed on a regular triangular lattice with 3 cm spacing between the centers of two nearest neighbors. This distance $L_{nn}(t)$, averaged over all the 19 large spheres, is measured in real time [22]. For a clear characterization of the segregation the mean value of the distance between nearest neighbors in the asymptotic regime, L_∞, is measured as a function of the filling fraction μ. Here, a transition between a non-segregated state at low density and a segregated state at high density can be defined. Since both transitions depend on the shaker amplitude we explored this dependence further. Fig. 6 shows the resulting phase diagram of the critical filling fractions $\mu_{c,seg}$ and $\mu_{c,ls}$, respectively, vs. shaker amplitude A. These critical filling fractions seem to be

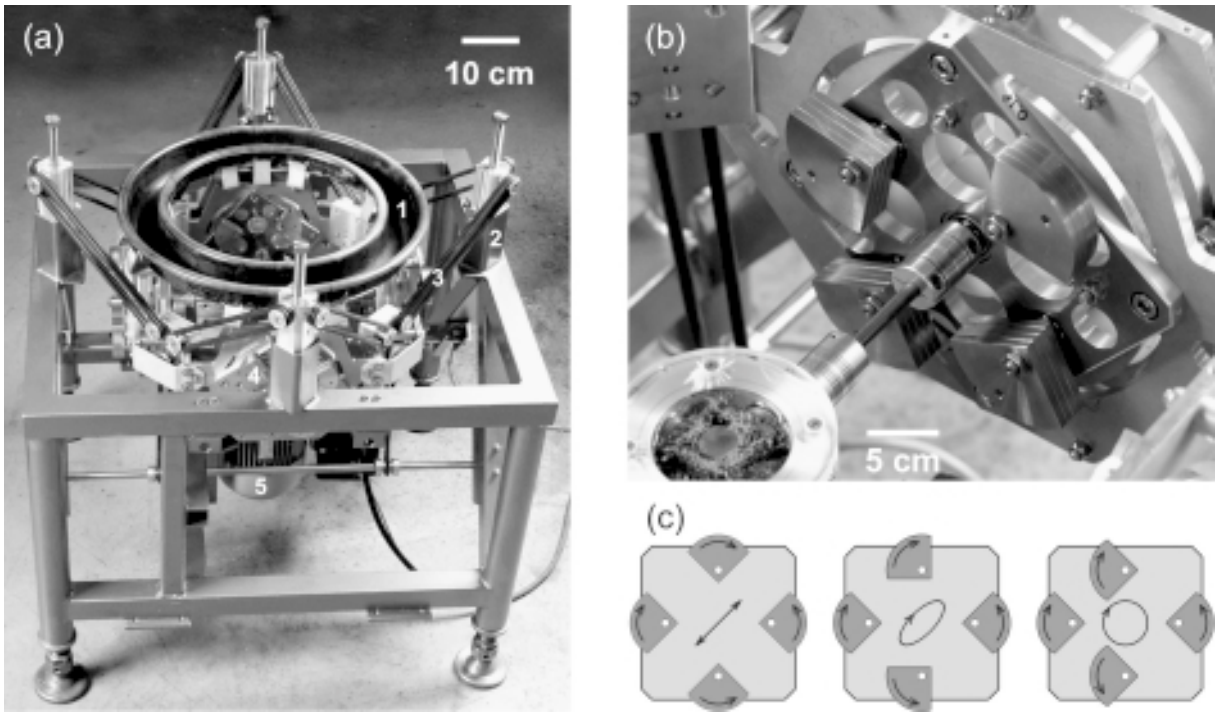

Fig. 7. (a) Annular conveyor: (1) Torus-shaped vibration channel, (2) Adjustable support, (3) Elastic band, (4) Vibration module with unbalanced masses, (5) Electric motor with integrated frequency inverter. (b) Driving module with four unbalanced masses. (c) Principle modes of oscillation: linear, elliptic, and circular.

independent on the driving frequency but decrease with increasing shaker amplitude. The regime where segregation occurs is always slightly above the liquid-solid transition line. This suggests that the granular phase transition is a precondition for segregation.

The transition is in the regime from 0.55 to 0.75 and depends on the amplitude of the driving shaker in a counterintuitive way: the liquid-solid transition line can be crossed by increasing the amplitude and thereby the energy input. A similar phenomenon was coined “freezing by heating” in the context of driven mesoscopic systems [23].

We offer the following thoughts to elucidate the connection between the segregation in the binary mixture and the phase transition in the monodisperse layer of spheres. It seems that the granular material does not stay uniformly distributed but chooses the configuration which minimizes the energy input for a given number of particles and excitation parameters, in order to reduce the amount of energy to be dissipated. For $\mu \leq \mu_c$ all particles move randomly with a uniform distribution, i.e., they prefer not to collide with the lateral wall. Indeed at low densities only few particle-wall collisions can be observed. We have measured that, in this case, large and small particles roll inside the dish in almost the same fashion. No segregation occurs. On the other hand, if the filling fraction exceeds μ_c, a boundary-hitting regime begins. This change can be seen and even heard in the experiment. In this regime the granules are continuously hit by the lateral wall. This process tends to decrease the extension of the monolayer which organizes itself in a more and more condensed state, leading to a triangular lattice, when the excitation is increased even further. Following the ideas of Edwards *et al.* [24], this is also the reason why segregation occurs: beyond the critical filling fraction the collisions with the lateral wall become the dominant driving mechanism. The granular material is continuously compressed by the collisions with the lateral wall and therefore tends to increase its compactness by organizing itself in a triangular lattice. Since the larger particles disturb this ordering process the system pushes these intruders into the central region of the dish thereby reducing the number of holes and defects [25,26].

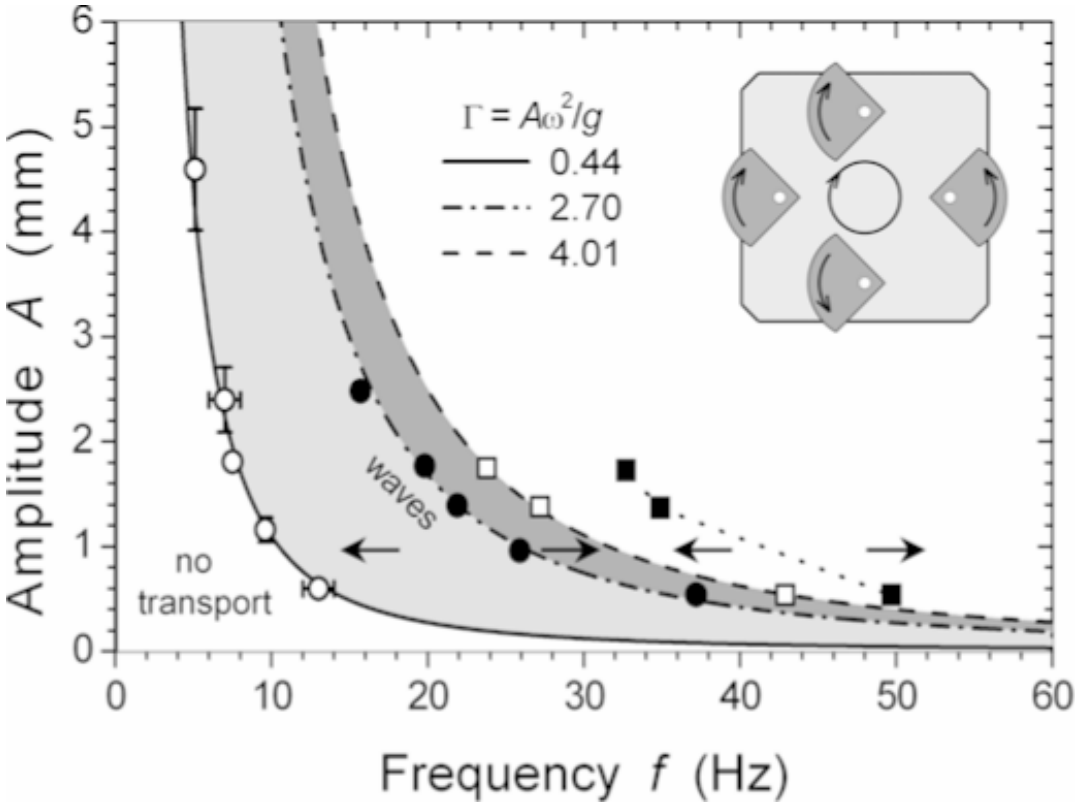

Fig. 8. Phase diagram of the transport behavior at circular forcing. The alternating arrows correspond to the transport direction with clockwise circular forcing.

We conclude that the main mechanism for size segregation in our binary system is the compression force exerted by the lateral boundary and mediated by the developing lattice of the smaller spheres.

4. VIBRATORY CONVEYOR

The combined action of vertical and horizontal vibration of the support has been utilized already for a long time for the controlled transport of bulk cargoes in a whole variety of industrial processes [27-29]. So-called “vibratory conveyors” are well established in routine industrial production for controlled transport of bulk solids. The transported goods can thereby be moved through three different mechanisms in the desired direction:

- sliding of the particles by asymmetric horizontal vibration (“gliding principle”),
- ballistic trajectories of the particles caused by inclined linear oscillation (“throw principle”), and
- horizontal transport through vertical vibration of a support with an asymmetric saw tooth profile of the base (“ratchet principle”).

Because of the complicated interactions between the vibrating trough and the bulk solids both glide and throw movements of the particles frequently appear within one oscillation cycle. Apart from the amplitude and frequency, the trajectory form of the conveyor’s motion also exerts an influence. Therefore it would be desirable to acquire a thorough knowledge of the dependence of the transport behavior on the three principle oscillation forms: linear, circular and elliptic.

First results from circular oscillations show granular surface waves in a certain range of frequencies. Such pattern formation and segregation phenomena have add in the past years to the interest of both engineers and physicists. It makes up the core problem of the discipline “Physics of Granular Material”. Using the vibratory conveyor, the question can be addressed: “How do structure formation and transport properties of granular material on vibrated surfaces influence each other?”

Through the construction of a ring-shaped vibrating channel, the long-time dynamics of a closed, mass conserving system devoid of distur-

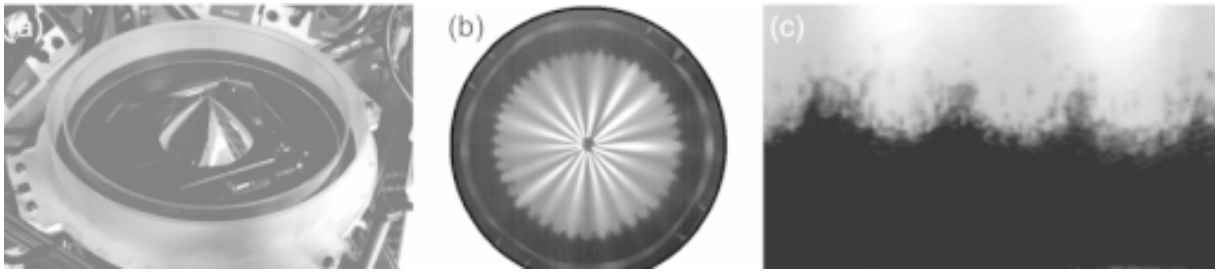

Fig. 9. (a) Experimental setup with transparent trough and conical mirror placed in the center of the ring. The reflected image of the surface profile is captured with a high-speed CCD camera on top of a mirror. (b) Anamorphotic image reflected from a conical mirror. (c) Section of a reconstructed granular surface.

bances from the influx and outpouring of grains can be studied. The main piece of the vibratory conveyor (c.f. Fig. 7a) is a torus-shaped vibrating channel of light-weight construction (carbon fiber strengthened epoxy) with an average diameter of 450 mm and a channel width of 50 mm. Firmly connected to the channel are four symmetrically arranged rotating vibrators. The complete oscillation system, the channel and drivers, are suspended with elastic bands in a highly adjustable frame.

The driving of the vibratory conveyor is done by an electric motor with integrated frequency inverter (SIEMENS Combimaster 1UA7). The above is connected via compensation clutches to the vibrators (see Fig. 7b). The excitation results from the simultaneous counter rotation of unbalanced masses, which are coupled with a gear. If two synchronously acting linear vibrators are oriented perpendicularly, then - through appropriate choice of the phase shift between the two - the shape of the vibration can be chosen and numerous Lissajous figures (linear, circular, elliptical) can be produced (see Fig. 7c). The phase can easily be adjusted through the choice of angle at which the unbalanced masses are mounted (for example 90 degrees for circular vibration).

For the first trial, the channel was loaded with 450 g of carefully sieved glass beads with mean diameter 1.1 mm. The layer thickness of the grains was about five particle diameters. The average transport speed was determined from the time of circulation of a colored tracer particle that the bulk carried along. This occurs automatically through a PC supported image processing system that detects the signal changes from the passing of the tracer through a row of the image and records the associated transit time.

Surprisingly, the mean transport direction depends, for circular agitation, on the amplitude A and frequency f in a characteristic manner (see Fig. 8). Below a critical value $\Gamma = 0.44$, the transport is impeded through static friction. Above this threshold, the bulk velocity initially increases before reaching its first maximum at $\Gamma = 1.1$, with half the circulation speed $A\omega$ of the circular motion. Increasing the excitation further leads to a deceleration of the granular flow, actually reversing its direction of motion in the range $2.70 < \Gamma < 4.01$. This alternating behavior repeats itself at still higher Γ.

Through application of five different unbalanced masses, the oscillation amplitude A can be varied between 0.53 mm and 2.35 mm. It is found that the conveyor speed increases linearly with the amplitude. The critical machine numbers Γ, at which the transport behavior changes qualitatively, are independent of the oscillation amplitude, at least for $\Gamma < 5$. In the frequency-amplitude parameter space (see Fig. 8) the threshold values lie on f^2 hyperbola of constant acceleration (“isoepitachs”).

For industrial applications, this observed reversal effect is relevant as the direction of a granular flow can be selected through the frequency of the excitation alone. One can employ such two-way conveyors for example in larger cascading transport systems as control elements to convey the material to different processes as needed.

5. GRANULAR SURFACE WAVES

The first appearance of a pattern in the grains can be observed at $\Gamma = 2.4$. The surface of the particles is then no longer flat, but rather shows peri-

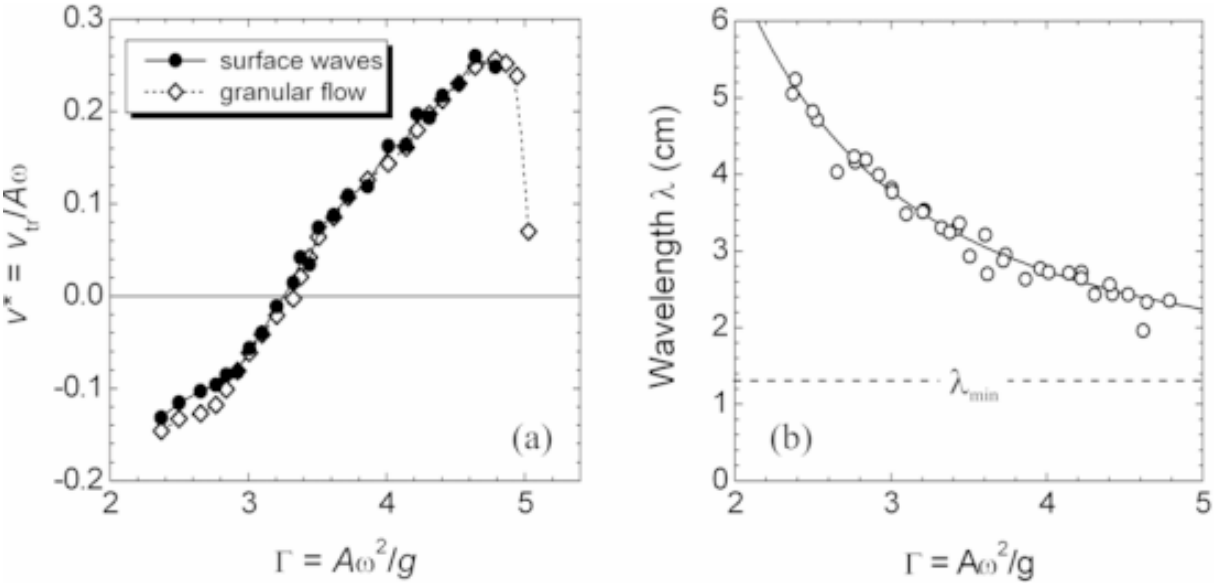

Fig. 10. (a) Scaled velocity v^* of surface waves and granular flow. (b) Circles represent the measured wavelength λ plotted over the normalized acceleration Γ. Throughout the measurement the driving amplitude was kept constant at 1.47 mm. The solid line is the graph of the function $\lambda = 1.3\text{cm} + 20\text{cm}\cdot\Gamma^{-1.9}$, the best fit to the data.

odic maxima and minima, quickly oscillating up and down (see Fig. 1b). Similar phenomena, namely standing waves in purely vertically shaken granular material, have been already observed [30,31]. In the system presented here, because of the symmetry breaking through the circular driving of the vibratory conveyor, these surface waves are traveling and therefore influence the bulk velocity. For the intended studies, the periodic boundary conditions of the channel geometry make it easier to analyze the topology of the surface waves by means of a Fourier spectrum of waves.

For comparison with theoretical models it is necessary to determine the dynamic surface profile $h(\varphi,t)$ during the transport process with high spatial and temporal resolution. This task has been solved by Pak and Behringer [32] only for a small section of an annular trough. Our container consists of a 2 cm wide annular channel with open top, 7 cm high Plexiglas walls, and a radius of R = 22.5 cm giving a circumference of L_0 =141 cm (see Fig. 9a). The granular system is observed from the top via a conical mirror placed in the center of the ring, similar to Ref. [32]. Thus a side view of the whole channel is captured with a single high-speed digital camera (resolution: 1280×1024 pixels at rates up to 500 images per second). Fig. 9b shows an anamorphotic image reflected from the conical mirror. The wavy granular surface is seen as a jagged ring around the tip of the cone. For reconstructing the true shape of the profile $h(\varphi,t)$ digital image processing is performed which delivers 360° panoramic side views of the granular profile in the channel. A small section of such a reconstructed granular surface is presented in Fig. 9c. The spatial resolution is sufficient for detecting single particles of 2 mm size. The channel is lit from outside through diffusive parchment paper wrapped around the outer wall, hence particles appear dark in front of a bright background.

If Γ exceeds 1, the vertical component of the circular acceleration will cause the grains to detach from the bulk followed by a flight on a ballistic parabola. This results in a much less dense-packed, *fluidized*, state with highly mobile constituents. In a certain driving range between $\Gamma_1 \approx 3.3$ and $\Gamma_2 \approx 3.7$ a locking of the time-of-flight between successive bounces and the period of the circular vibration occurs [34]. The initially flat bed becomes destabilized, and undulations of the granular surface occur in the range $2.4 < \Gamma < 4.5$ [35,36]. High-speed CCD imaging showed that they oscillate with half the excitation frequency ("*f*/2 waves"). As mentioned, in contrast to previous work [32, 37-39] done

at purely vertical vibration the present waves are not stationary but are transported along the annular trough. The drift velocity of the wave pattern can be measured by applying a phase-locked imaging technique with fixed time delay $\Delta t = 2T$. This is done with a camera which is triggered by a pick-up signal taken from the rotating unbalanced masses. From these images space-time diagrams can be constructed. The deviation of the striped pattern from the vertical is taken as a measure for the wave speed.

A comparison of the wave speed with the bulk velocity of the transported particles shows that both velocities are identical (Fig. 10a). In particular, a reversal of the wave velocity is also possible by adjusting the vibration frequency alone. In the range $\Gamma \approx 4.5$, when the granular flow is reversed a second time, surface waves disappear. The granular surface becomes flat but still oscillates at twice the vibration frequency. Above $\Gamma \approx 5.5$ standing waves are observed again but this time repeating their patterns after four shaker periods ("*f*/4 waves"). This scenario is reminiscent to the wave patterns found by Bizon *et al.* [39] for vertical vibration of a laterally extended system.

A more detailed analysis of the Γ dependence of the wave length λ shows

$$\lambda(\Gamma) = \lambda_{min} + \Lambda \cdot \Gamma^{\alpha}, \qquad (4)$$

see Fig. 10b. For the minimum wavelength λ_{min} we obtain a value of 1.3 ± 0.3 cm, which is approximately the depth of the granular layer. The values for the other parameters are Λ = 20 ± 4 cm and α = -1.9 ± 0.3. This is consistent with the results of Metcalf *et al.* [30] who examined the dependence of the wavelength on the peak acceleration Γ at constant frequency.

6. CONCLUSIONS

To summarize, the vibratory systems presented here have demonstrated their potential for the investigation of the pattern formation and transport properties of granular materials in a systematic way. Considering the granular pattern formation, the described annular apparatus is unrivaled for its capability to study solid-liquid transitions since, due to the permanent transport of all particles at periodic boundary conditions, the influence of spatial inhomogeneities is excluded:

- propagating patterns which persist along the whole system cannot be caused by local inhomogeneities of the container and
- one can wait until any transient due to coarsening processes of the developing patterns have disappeared.

For a further understanding of the general behavior of granular material on vibratory conveyors the next steps are

- the development of a better understanding of *segregation phenomena* in multidisperse systems,
- the investigation of *clustering patterns* in submonolayers, and
- the qualitative modelling of the *spatiotemporal surface structure*.

ACKNOWLEDGEMENTS

We would like to thank A. Aumaître, A.P.J. Breu, R. Brito, H. El hor, H.-M. Ensner, A. Götzendorfer, R. Grochowski, F. Landwehr, S.J. Linz, J. Kreft, I. Rehberg, M. Rouijaa, T. Schnautz, M. Schröter, S. Strugholtz, D. Svenšek, and P. Walzel for valuable discussions.

Support by Deutsche Forschungsgemeinschaft (DFG-Sonderprogramm "Verhalten granularer Medien", Kr1877/2) is gratefully acknowledged.

REFERENCES

[1] H.M. Jaeger, S.R. Nagel and R.P. Behringer // *Rev. Mod. Phys*. **68** (1996) 1259.
[2] L.P. Kadanoff // *Rev. Mod. Phys*. **71** (1999) 435.
[3] K.M. Hill and J. Kakalios // *Phys. Rev*. E **49** (1994) R3610.
[4] J. Duran, J. Rajchenbach and E. Clement // *Phys. Rev. Lett*. **70** (1993) 2431.
[5] P.M. Reis and T. Mullin // *Phys. Rev. Lett*. **89** (2002) 244301.
[6] E. Falcon, R. Wunenburger, P. Evesque, S. Fauve, C. Chabot, Y. Garrabos and D. Beysens // *Phys. Rev. Lett*. **83** (1999) 440.
[7] G. Strassburger and I. Rehberg // *Phys. Rev*. E **62** (2000) 2517.
[8] J.C. Williams // *Powder Tech*. **15** (1976) 245.
[9] J.B. Knight, H.M. Jaeger and S.R. Nagel // *Phys. Rev. Lett*. **70** (1993) 3728.
[10] M.E. Möbius, B.E. Lauderdale, S.R. Nagel and H.M. Jaeger // *Nature* **414** (2001) 270.
[11] M. Medved, H.M. Jaeger and S.R. Nagel // *Phys. Rev*. E **63** (2001) 061302.
[12] A. Rosato, K.J. Strandburg, F. Prinz and R.H. Swendsen // *Phys. Rev. Lett*. **58** (1987) 1038.
[13] R. Jullien, P. Meakin and A. Pavlovitch // *Phys. Rev. Lett*. **69** (1992) 640.

[14] T. Shinbrot and F.J. Muzzio // *Phys. Rev. Lett*. **81** (1998) 4365.
[15] D.C. Hong, P.V. Quinn and S. Luding // *Phys. Rev. Lett*. **86** (2001) 3423.
[16] N. Shishodia and C.R. Wassgren // *Phys. Rev. Lett*. **87** (2001) 084302.
[17] J.A. Both and D.C. Hong // *Phys. Rev. Lett*. **88** (2002) 124301.
[18] D.C. Hong // *Physica* A **271** (1999) 192.
[19] A.P.J. Breu, H.-M. Ensner, C.A. Kruelle and I. Rehberg // *Phys. Rev. Lett*. **90** (2003) 014302.
[20] A. Götzendorfer, C.-H. Tai, C. A. Kruelle, I. Rehberg and S.-S. Hsiau // *Phys. Rev*. E **74** (2006) 011304.
[21] S. Aumaître, T. Schnautz, C.A. Kruelle and I. Rehberg // *Phys. Rev. Lett*. **90** (2003) 114302.
[22] S. Aumaître, C.A. Kruelle and I. Rehberg // *Phys. Rev*. E **64** (2001) 041305.
[23] D. Helbing, I.J. Farkas and T. Vicsek // *Phys. Rev. Lett*. **84** (2000) 1240.
[24] S.F. Edwards and D.V. Grinev // *Phys. Rev*. E **58** (1998) 4758.
[25] A.D. Dinsmore, A.G. Yodh and D.J. Pine // *Phys. Rev*. E **52** (1995) 4045.
[26] J. Duran and R. Jullien // Phys. Rev. Lett. **80** (1998) 3547.
[27] G. Pajer, H. Kuhnt and F. Kuhnt, *Fördertechnik - Stetigförderer* (VEB Verlag Technik, Berlin, 1988).
[28] F.J.C. Rademacher and L. Ter Borg // *Eng. Res*. **60** (1994) 261.
[29] E.M. Sloot and N.P. Kruyt // *Powder Technol*. **87** (1996) 203.
[30] T. Metcalf, J.B. Knight and H.M. Jaeger // *Physic*a A **236** (1997) 202.
[31] P.B. Umbanhowar, F. Melo and H.L. Swinney // *Physica* A **249** (1998) 1.
[32] H.K. Pak and R.P. Behringer // *Phys. Rev. Lett*. **71** (1993) 1832.
[33] E. van Doorn and R.P. Behringer, In: *Powders and Grains 1997*, ed. by R.P. Behringer and J. Jenkins (Balkema, Leiden 1997), p. 397.
[34] F. Melo, P.B. Umbanhower and H.L. Swinney // *Phys. Rev. Lett*. **75** (1995) 3838.
[35] C.A. Kruelle, S. Aumaître, A.P.J. Breu, A. Goetzendorfer, T. Schnautz, R. Grochowski and P. Walzel,In: *Advances in Solid State Physics* **44,** ed. by B. Kramer (Springer, Berlin 2004), p. 401.
[36] A. Götzendorfer, C.A. Kruelle and I. Rehberg, In: *Powders and Grains 2005*, ed. by R. García-Rojo, H.J. Herrmann and S. McNamara (Balkema, Leiden 2005), p. 1181.
[37] S. Douady, S. Fauve and C. Laroche // *Europhys. Lett*. **8** (1989) 621.
[38] F. Melo, P. Umbanhowar and H.L. Swinney // *Phys. Rev. Lett.* **72** (1994) 172.
[39] C. Bizon, M.D. Shattuck, J.B. Swift, W.D. McCormick and H.L. Swinney // *Phys. Rev. Lett*. **80** (1998) 57.
[40] J. Kepler, *Strena Seu De Niue Sexangula* (G. Tampach, Francofurti, 1611).